

IMPROVED DISASTER MANAGEMENT THROUGH POST-EARTHQUAKE BUILDING DAMAGE ASSESSMENT USING MULTITEMPORAL SATELLITE IMAGERY

B. J. Adams^{a, *}

^a ImageCat, Inc. 400 Oceangate, Suite 1050, Long Beach, California, 90802, USA –

Commission VII, WG VII/5

KEY WORDS: Earthquakes, Decision Support, Change Detection, Multitemporal, High resolution, Optical, SAR

ABSTRACT:

Remote sensing technology is playing an increasingly important role in post-disaster decision support. Organizations including the Earthquake Engineering Research Institute (EERI) and Multidisciplinary Center for Earthquake Engineering Research (MCEER) recognize that following major earthquakes, satellite imagery can bring significant benefits to response and recovery efforts, through urban damage assessment. Following an introductory review of prior research undertaken in the field, this paper presents methodological techniques for determining the location and severity of post-earthquake building damage. The damage detection algorithms are based on the comparative analysis of a multitemporal sequence of optical or SAR images, acquired before and after the event. Following initial pre-processing to geo-reference and co-register the imagery, damage is detected in terms of spectral changes between the scenes. Depending on its spatial resolution, image processing techniques including edge detection and texture analysis may then be used to isolate features of interest within the coverage. Change is subsequently quantified with a range of arithmetic operators. Damage location is visualized using damage maps, and severity expressed graphically as damage profiles. The efficacy of these analytical procedures is demonstrated with respect to the Marmara (Turkey) earthquake of August 17th 1999, for which 10m panchromatic SPOT 4 and 20m SAR ERS coverages were available. Preliminary results are also presented for the May 21st, 2003 Boumerdes earthquake in northern Algeria, where 60cm Quickbird imagery was acquired. In this latter case, the change detection algorithms offer a quick-look region-wide damage assessment, providing the focus for more detailed visual inspection of building damage on a per-structure basis. The development of damage profiles for Boumerdes is an ongoing research topic. In future earthquakes, these techniques could guide the work of field reconnaissance teams; support the prioritization of relief efforts; direct search and rescue teams to victims; facilitate loss estimation; and help determine whether the situation warrants international aid.

1. INTRODUCTION

The use of remote sensing technology is, for a number of reasons, becoming increasingly widespread following natural disasters. On a policy level, international initiatives such as the 2000 Charter on Space and Major Disaster (International Charter, 2003) constitute a significant commitment towards the use of space facilities for emergency management. In terms of data accessibility, programs including the ESA Earth Watching Service now freely distribute satellite disaster coverage (ESA, 2003). Remote sensing also has a proven track record in the aftermath man-made events like the World Trade Center attack (Huyck and Adams, 2002) and Columbia space shuttle disaster (NOAA, 2003). These factors, combined with investment in applied research from organizations such as the Multidisciplinary Center for Earthquake Engineering Research (MCEER), are facilitating its deployment through progressive end-users, like the Earthquake Engineering Research Institute (EERI) reconnaissance team (see Adams *et al.*, 2004).

In the case of post-earthquake urban damage assessment, remotely sensed data offers significant advantages over traditional methods of field survey – it is low-risk, and offers a rapid overview of building collapse across an extended geographic area. Accordingly, damage detection techniques are now appearing in the literature, employing either indirect or direct methodological approaches. In the former instance, urban damage is inferred from a surrogate measure such as night-time lighting levels (Hashitera *et al.*, 1999 and Kohiyama *et al.*, 2001). In the latter, building damage is recorded directly, based

on its distinctive signature within the imagery (for details, see Matsuoka and Yamazaki, 1998; also Chiroiu *et al.*, 2002). Direct approaches may be categorized as mono- and multitemporal. Monotemporal analysis detects damage in imagery acquired after the disaster has occurred (Ogawa and Yamazaki, 2000; Hasegawa *et al.*, 2000; Chiroiu and Andree, 2001; Mitomi *et al.*, 2002). The multitemporal technique instead assesses damage based on spectral changes between images acquired at several time intervals; typically ‘before’ and ‘after’ an extreme event.

The following paper presents a multitemporal change detection algorithm (see also Eguchi *et al.*, 2000) for determining the location and severity of post-earthquake building damage. Section 2 introduces the methodological approach, while Section 3 describes its implementation for the 1999 Marmara (Turkey) and recent 2003 Boumerdes (Algeria) earthquake. Discussion and conclusions are presented in Section 4.

2. METHODOLOGICAL APPROACH

The flow chart in Figure 1 introduces the basic damage detection methodology for optical and SAR satellite imagery. The pair of ‘before’ and ‘after’ images is pre-processed to remove geometric errors inherent in the data, and register all scenes to a common coordinate system. Depending on the sensor resolution, an additional image processing step involving edge detection and texture analysis may then be performed, highlighting features of interest (i.e. non-damaged and collapsed buildings). Changes between the scenes are then

* Corresponding author.

computed using a simple arithmetic operator, such as the difference, correlation or block correlation. The location of building damage is displayed using a damage assessment map. Damage severity is established through building damage profiles, which demonstrate the general association between temporal changes in the remote sensing coverage and the extent of building collapse (as determined by field survey).

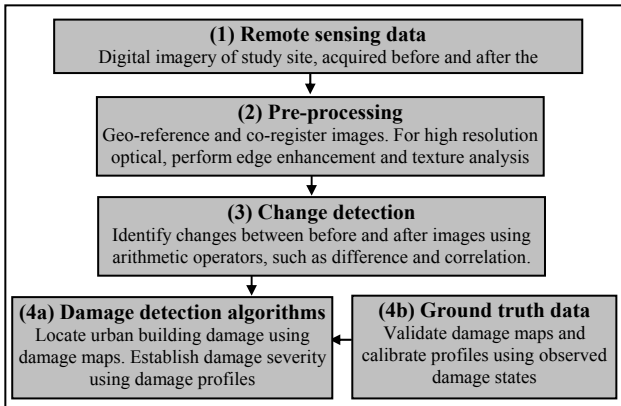


Figure 1. Building damage detection methodology

3. IMPLEMENTATION

3.1 1999 Marmara (Turkey) earthquake

3.1.1 Method: Change detection algorithms were developed for the Turkish city of Golcuk, the most densely populated settlement in Kocaeli province. As illustrated in Figure 2, the city experienced extensive damage during the 17th August 1999 magnitude 7.4 earthquake. According to Coburn *et al.* (1999, cited in Rathje, 2000), 30-40% of structures collapsed, due mostly to pancaking and the soft first story effect.



Figure 2 Building damage in Golcuk (courtesy of R. Andrews)

As shown in Table 1, remotely sensed SPOT 4 panchromatic and ERS intensity and complex images were acquired 'before' and 'after' the earthquake. In terms of pre-processing, the respective datasets were geo-referenced and co-registered. The SPOT imagery was provided in a geo-referenced format, and the scenes co-registered within the ENVI processing environment. For the SAR coverage, ground control points were extracted using the ESA SAR Toolbox, with geo-referencing performed in ENVI. The co-registration was fine tuned by applying a template matching algorithm.

Earthquake	Sensor	Spatial Resolution (m)	Date
Marmara	SPOT 4 (pan)	10	Before: 7/15/99 After: 8/20/99
	ERS 2 ERS1	20	Before: 4/24/99 After: 9/10/99
Boumerdes	Quickbird (pan and MS)	0.6 and 2.4	Before: 4/22/02 After: 5/23/03

Table 1. Remote sensing imagery specifications

The performance of several change detection measurements was investigated. For the SPOT panchromatic data: (1) simple difference (dif); (2) sliding window-based (cor) correlation; and (3) modulated block correlation (bk_cor), were computed between the 'before' and 'after' images. In the case of SAR intensity and complex data, indices comprised: (1) simple difference between intensity values; (2) sliding window-based correlation; (3) modulated block correlation; and (4) coherence (coh) or complex correlation between complex images.

The next methodological step compares indices of change with 'ground truth' damage data collected shortly after the earthquake by the Architectural Institute of Japan reconnaissance team (AIJ, 1999). The zone-based sampling strategy in Figure 3a was employed, using 70 administrative boundaries corresponding with the street network. Within each zone, damage states were recorded for a sample of buildings using the European Macro-seismic Scale (EMS98):

- Grade 1: Negligible to slight damage
- Grade 2: Moderate damage
- Grade 3: Substantial to heavy damage
- Grade 4: Very heavy damage
- Grade 5: Destruction/collapse

The corresponding damage state map in Figure 3b expresses the percentage of collapsed structures (Grade 5) as a function of the total number of observations (sum of Grade 1 through Grade 5). For analytical purposes, these percentages are divided into the following categories: A (0-6.25% of buildings totally collapsed); B (6.25-12.5%); C (12.5-25%); D (25-50%); and E (50-100%). The additional 'Sunk' zone corresponds with an area in north-east Golcuk experiencing significant subsidence.

Finally, damage maps and building damage profiles were generated to determine the location and severity of urban damage. For the profiles, average change was computed for each of the 70 zones, and these responses aggregated by damage state. The result is a central measure of tendency and standard deviation (plotted as error bars) for class A through class E.

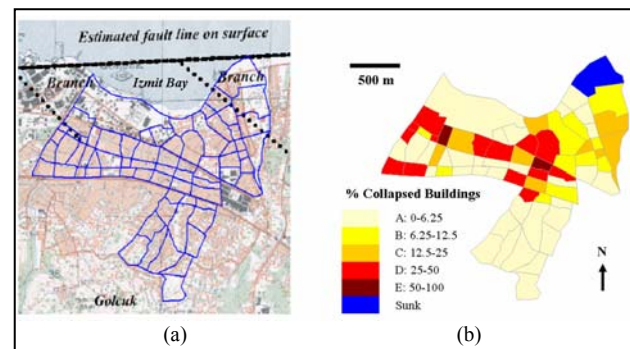


Figure 3. (a) Delineation of the 70 sample zones in Golcuk. (b) Ground observations of building collapse (AIJ, 1999)

3.1.2 Damage location: Figure 4 depicts damage maps for Golcuk, obtained using the various measures of change. The difference scene in Figure 4a is classified to highlight regions of Golcuk exhibiting pronounced differences in reflectance. Changes are concentrated in the city center, with strongly negative values suggesting a marked increase in reflectance following the earthquake. With reference to the damage map in Figure 3b, these areas correspond with zones of severe building damage (categories D-E). This result suggests that debris

associated with collapsed buildings exhibits a higher spectral return than the standing structure. Although considerable damage was also sustained in western Golcuk, reduced differences may be due to suppressed reflectance values where smoke from the burring Tupras oil refinery was present in the upper atmosphere. Positive differences are limited to the ‘Sunk’ coastal stretch, where reflectance values have fallen following widespread inundation.

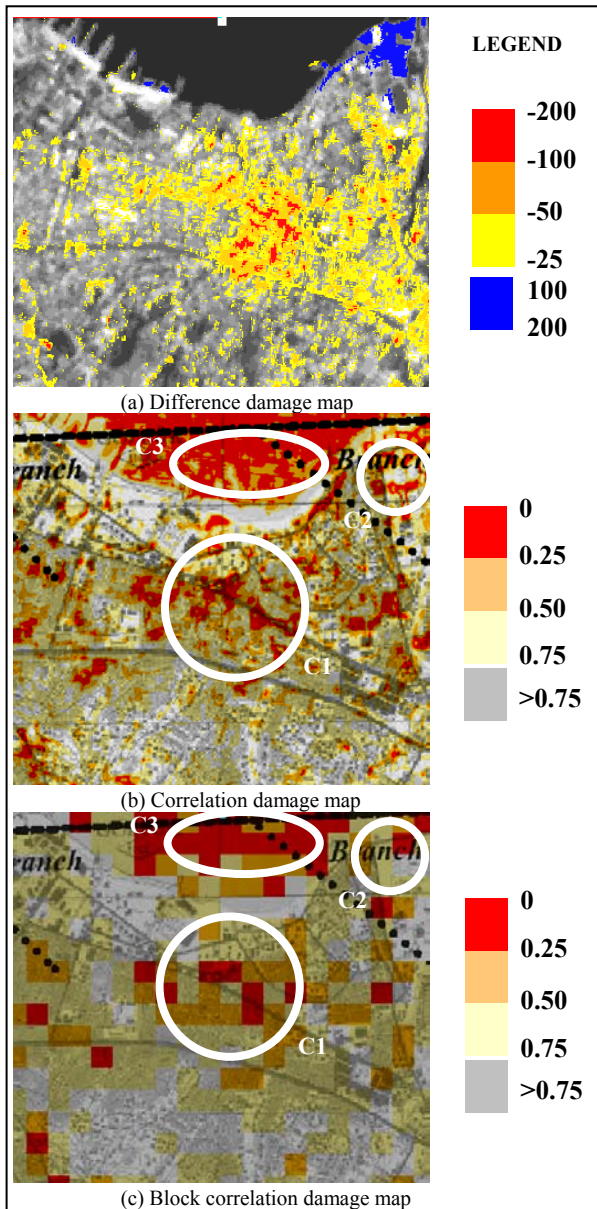


Figure 4 SPOT damage maps. Areas of high positive difference and low correlation correspond with the Golcuk city center, which from Figure 3b sustained severe and widespread building damage. See text for explanation of annotations C1-C3.

Results for the block and window-based correlation (Figure 4b and Figure 4c) are overlaid with a base map of Golcuk. For visualization purposes, all values are displayed as positive, since the magnitude rather than the direction of change is of interest. For both block and sliding window-based results, areas of low correlation (displayed in red) are concentrated in central Golcuk (see annotation C1). As for the difference values, the damage map in Figure 3b confirms that building collapse was widespread. A low level of correlation around the subsidence

zone (C2) is due to the change in reflectance following inundation. Low correlation offshore (C3) is probably attributable to the random or chaotic patterns of surface reflectance associated with wind-driven wave action.

Figure 5 depicts the SAR intensity responses for Golcuk. For visualization purposes, the difference image in Figure 5a was thresholded at $-7.0 < dif < 7.0$, with intermediate values displayed across an 8-bit range using a linear contrast stretch. Similarly, correlation images in Figure 5b and Figure 5c were thresholded at $0.2 < cor < 0.6$. Block correlation statistics were further classified into categories of: low ($0 < bk_cor < 0.2$); moderate ($0.2 < bk_cor < 0.4$); high ($0.4 < bk_cor < 0.6$); and very high ($bk_cor > 0.6$). The coherence image in Figure 5d was thresholded at $0.3 < coh < 0.6$.

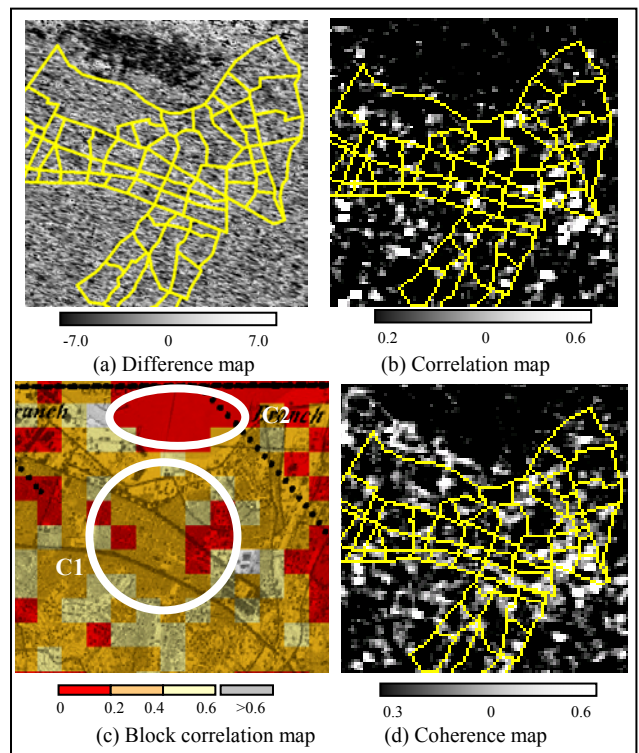


Figure 5 SAR damage maps. Areas of low correlation correspond with Golcuk city center, which from Figure 3b sustained severe and widespread building damage. See text for explanation of annotations C1-C2

From Figure 5a, the magnitude of SAR intensity difference is low compared with its optical counterpart. It is difficult to discern any obvious regularity in response, with the urban centre exhibiting an amalgam of positive and negative values. Low correlation (see annotation C1 in Figure 5c) is evident throughout central areas of Golcuk. Once again, this corresponds with high levels of building collapse (Figure 3b). Low correlation outside the urban area is concentrated around Izmit Bay (C2), where changing water surface conditions cause differences in backscatter. In Figure 5d, low coherence is present throughout both urban and rural areas, suggesting that this measure has limited ability to distinguish earthquake building damage from other modes of change.

3.1.3 Damage severity: From the zone-based damage profiles in Figure 6, panchromatic imagery yields an encouraging trend between difference and damage state (Figure 6a). As the percentage of collapsed buildings increases from class A to E,

the offset between ‘before’ and ‘after’ scenes widens. For category A, where 0-6.25% of structures collapsed, values tend towards zero. In contrast, dif \sim -50DN for category E (50-100% building collapse). The positive difference of dif \sim 80DN for the ‘Sunk’ category confirms that damage profiles distinguish between types of earthquake-related damage. In the SPOT correlation profiles (Figure 6b and Figure 6c) values decrease as the degree of building damage increases from class A to class E. These trends again suggest that the transition from stranding structures (‘before’) to debris (‘after’) produces a distinct signature throughout visible regions of the spectrum.

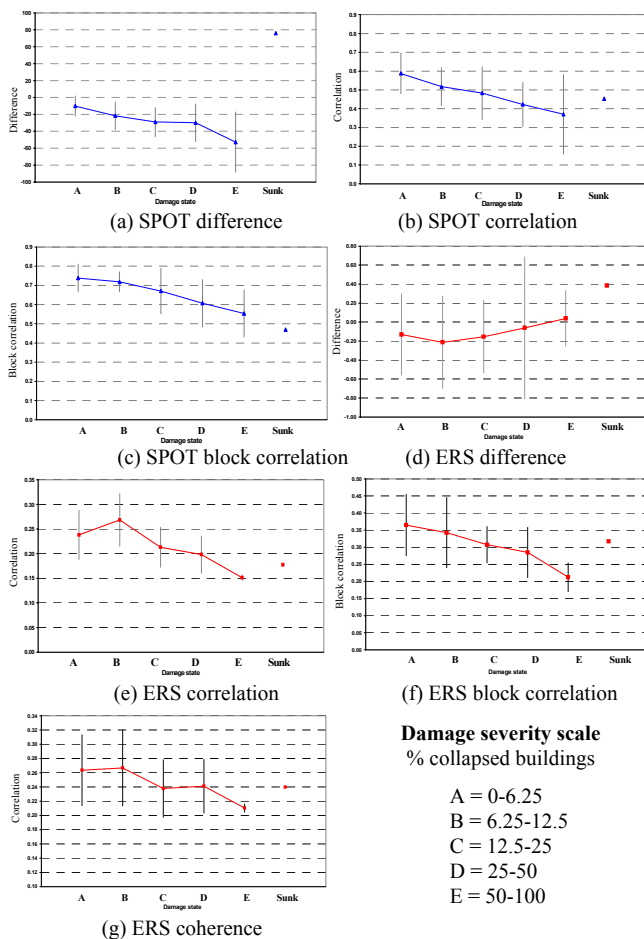


Figure 6 Damage profiles for Golcuk, showing how indices of change vary with the severity of building collapse

The SAR intensity difference profile in Figure 6d exhibits an upward trend, as the percentage of collapsed structures increases with the transition from category A to E. In absolute terms, the change in intensity is negative for zones experiencing minor damage, and tends towards zero as the percentage of collapsed structures reaches a maximum for class E. These values are contrary to expectation. In theory, reduced backscatter accompanying building collapse would yield a positive difference, as return from the ‘after’ scene is lower than ‘before’. However, returning to the constituent intensity images, negative values for A-D arise because backscatter is consistently higher throughout the ‘after’ scene. This baseline offset is independent of earthquake damage, and is instead attributable to varied conditions at the times of imaging, due to weather effects and possibly look angle. Values for class E tend towards zero, because the offset due to building collapse is largely mitigated by a universal reduction in backscatter.

The sliding window and block statistical approaches (Figure 6e and Figure 6f) reveal the same tendency as SPOT data; mean correlation decreases as building damage escalates. Thus, correlation provides a consistent association between temporal changes on remote sensing imagery and urban building damage. The coherence profiles in Figure 6g exhibit a similar pattern of response, although the degree of change is lessened.

3.2 2003 Boumerdes (Algeria) earthquake

3.2.1 Method: Change detection algorithms were developed for the Algerian city of Boumerdes, located some 50km east of the capital Algiers. After the 6.8 magnitude earthquake struck on May 21st 2003, Boumerdes was among the worst-affected cities. Building damage was widespread (see Figure 7; also Adams *et al.*, 2003), with an estimated 150,000 people displaced from their homes (OCHA, 2003).

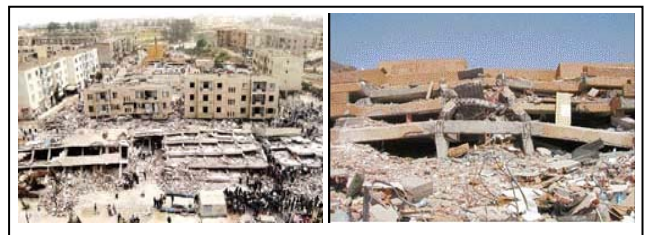


Figure 7 Building damage in Boumerdes (courtesy of AP Photo and EERI)

Table 1 provides details of the optical Quickbird images acquired ‘before’ and ‘after’ the earthquake. Provided by DigitalGlobe in geo-referenced format, the scenes were co-registered using ENVI software. This registration process largely mitigated a fundamental geometric offset between the scenes, in the order of 5m.

Exploratory data analysis, following the same approach employed for the Marmara earthquake, suggested that the increase in spatial resolution to 60cm warranted an adjustment to the change detection methodology. Differencing and correlation of the panchromatic bands on per-pixel basis produced high levels of noise, from which earthquake-related changes were indistinguishable. The extraneous intensity changes are probably due to a variation in sensor look angle and the temporal interval of 13 months between data acquisition. To isolate spectral changes associated with urban damage, edge detection and texture filters were applied to the panchromatic scenes. The theory is that building collapse produces a distinct textural signature compared with non-damaged structures. This approach was not viable for the SPOT coverage of Marmara, since the textural characteristics of individual structures are indiscernible at 10m resolution.

To highlight edges associated with building collapse and debris, a Laplacian filter was applied in ENVI to each panchromatic image. Experimentation indicated that a 9x9 filter was optimal. Textural analysis was then performed for a suite of co-occurrence measures, including: mean; variance; homogeneity; contrast; dissimilarity; entropy; second moment; and correlation. Visual inspection of the results suggested that a 25x25 dissimilarity matrix most effectively distinguished structural collapse and accompanying debris from non-damaged buildings and changes unrelated to the earthquake. The resulting scenes were then differenced on a per-pixel basis. In

an effort to distinguish damage sustained by individual buildings, difference values were reclassified using ArcView GIS software, in terms of their standard deviation about the image mean. An average standard deviation was then computed within a 200x200 cell window (approximating the dimensions of Boumerdes residential structures). Mapping these block statistics in intervals of 1 standard deviation highlights areas of potential building collapse, where textural change is consistently high.

For the Boumerdes case study, the final stage of damage profile development has yet to be completed. This work will draw on the building damage interpretation performed by Chiba University, Japan (see Yamazaki *et al.*, 2003). The general distribution of collapsed buildings is shown in Figure 8. In the meantime, damage severity is assessed qualitatively, through detailed visualization of locations on the Quickbird imagery exhibiting extreme textural changes.

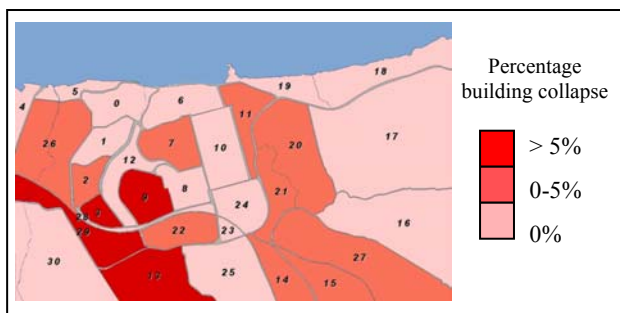


Figure 8 Distribution of building collapse in Boumerdes (courtesy of F. Yamazaki)

3.2.2 Damage location: In the Boumerdes damage map (Figure 9), areas depicted in red and yellow correspond with extreme textural changes accompanying building collapse. Concentrated damage in the south-west of the city corresponds with zones 3 and 9 in the Chiba results (Figure 8), where >5% of buildings collapsed. Extreme change within the coastal waters is probably attributable to textural variations in sea surface conditions.

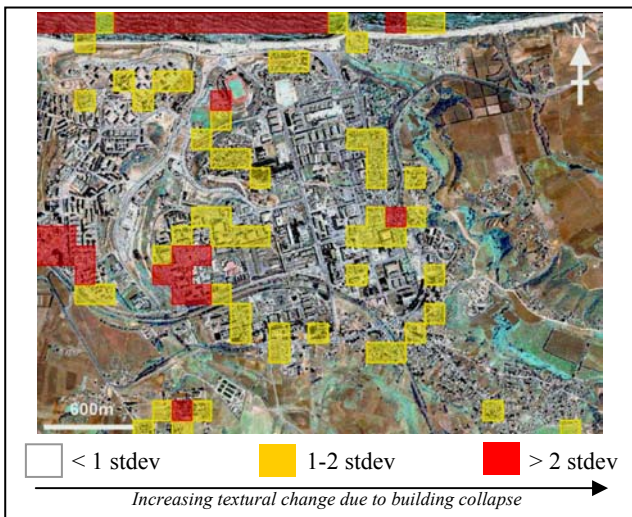


Figure 9 Quickbird damage map for Boumerdes. High average block standard deviation from the image mean corresponds with extreme textural changes caused by building collapse.

3.2.3 Damage severity: Figure 10 offers a detailed representation of neighbourhoods selected from Figure 9, as

regions of severe building damage. From visual inspection, significant structural and geometric irregularities are apparent. Collapsed apartment blocks are readily distinguished by the bright yet chaotic appearance of debris. Where buildings have pancaked or toppled sideways, changes in shape and position are also evident.

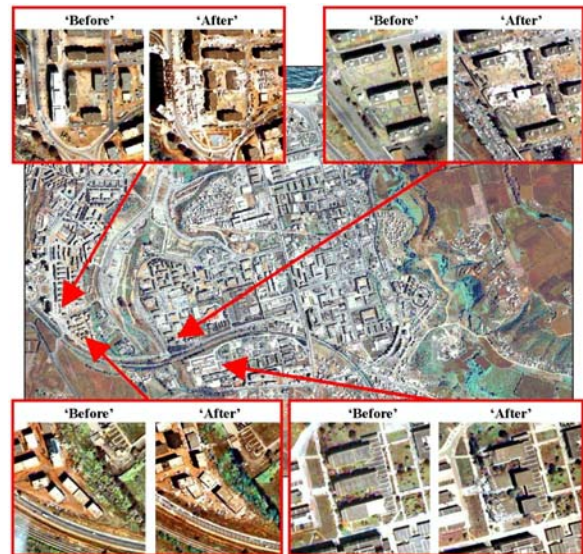


Figure 10 Visualization of building collapse in Boumerdes. The selected neighbourhoods were identified as regions of extreme textural change in the damage map (Figure 9)

4. DISCUSSION AND CONCLUSIONS

Results from the multitemporal change detection methodologies presented in this paper demonstrate that high resolution Quickbird and moderate resolution SPOT and ERS satellite imagery can be used to successfully determine the *location* and *severity* of post-earthquake building collapse.

Extreme negative differences in the SPOT panchromatic damage map for Golcuk confirms that building debris exhibits a higher (brighter) return than non-damaged structures. Trends are more difficult to discern in the SAR difference damage map, with temporal changes difficult to separate from seemingly arbitrary changes throughout the scene. Reduced values in SPOT and SAR correlation damage maps for central Golcuk, suggests that these measures are also sensitive to building collapse. Given the respective advantages of optical and radar imagery, namely ease of interpretation, and 24/7 all weather viewing, future integration of these measures through data fusion techniques, could improve the accuracy and robustness of building damage detection algorithms. To achieve further accuracy improvements, the occurrence of false positives should be reduced. The effectiveness of NDVI masking for eliminating anomalous changes due, for example, to vegetation seasonality or water surface effects, will be investigated.

Damage profile performance essentially mirrored the distinguishing potential of the Golcuk damage maps. For the SPOT imagery, simple subtraction and correlation profiles varied with damage severity. While SAR correlation indices also distinguished trends in the density of collapsed structures, the subtraction profile was instead dominated by radiometric offset between the 'before' and 'after' scenes. Introducing radiometric matching to the damage detection methodology could, to a large degree, overcome this limitation.

For the 2003 Boumerdes event, the increase in spatial resolution to 60cm necessitated additional processing, to distinguish damage associated with building collapse. When plotted as a damage map, the differenced edge detection and textural dissimilarity results successfully located blocks of extreme change. In this case, change was measured relatively rather than absolutely, in terms of the standard deviation about the image mean. The spectral signature of earthquake building damage differs around the World, as the building stock and construction materials vary. As such, devising universally applicable measures of change poses a considerable challenge. Future work will concentrate on standardising the methodology, so that buildings damage can be detected, irrespective of urban setting.

The damage detection methodology presented in this paper offers significant improvements to *disaster management*. It may be envisaged how damage maps could provide emergency responders and reconnaissance teams with a 'quick-look' regional damage assessment, supporting the prioritization of relief efforts, enabling loss estimation, and immediately determining whether the situation warrants international aid. In terms of search and rescue, inspection of damage severity through damage profiles and visual inspection could pinpoint collapsed structures where victims may be trapped.

5. REFERENCES

- Adams, B.J., Huyck, C.K. and Eguchi, R.T., 2003. The Boumerdes (Algeria) earthquake of May 21, 2003: Preliminary reconnaissance using remotely sensed data, <http://mceer.buffalo.edu/research/boumerdes/default.asp> (accessed 5 Feb. 2004)
- Adams, B.J., Huyck, C.K., Mio, M., Cho, S., Ghosh, S., Chung, H.C., Eguchi, R.T., Houshmand, B., Shinozuka, M., and Mansouri, B., 2004. The Bam (Iran) earthquake of December 26, 2003: Preliminary reconnaissance using remotely sensed data and the VIEWS system, <http://mceer.buffalo.edu/research/bam/default.asp> (accessed 5 Feb. 2004)
- AIJ, 1999. *Report on the Damage Investigation of the 1999 Kocaeli Earthquake in Turkey*. AIJ, Tokyo.
- Chiroiu, L. and Andre, G., 2001. Damage assessment using high resolution satellite imagery: application to 2001 Bhuj, India earthquake, <http://www.riskworld.com/Nreports/2001/Bhuj,India,earthquake2001.PDF> (accessed 5 Feb. 2004)
- Chiroiu, L., Andre, G., Guillande, R., and Bahoken, F., 2002. Earthquake damage assessment using high resolution satellite imagery, *Proceedings of the 7th National US Conference on Earthquake Engineering*, Boston.
- Eguchi, R., Huyck, C., Houshmand, B., Mansouri, B., Shinozuka, M., Yamazaki, F. and Matsuoka, M., 2000. *The Marmara Earthquake: A View from Space, The Marmara, Turkey Earthquake of August 17, 1999: Reconnaissance Report, Section 10, Technical Report MCEER-00-0001*, MCEER: Buffalo
- ESA, 2003. Earth Watching, <http://earth.esa.int/ew/> (accessed 5 Feb. 2004)
- Hasegawa, H., Yamazaki, F., Matsuoka, M. and Seikimoto, I., 2000. Determination of building damage due to earthquakes using aerial television images, *Proceedings of the 12th World Conference on Earthquake Engineering*, Auckland.
- Hashitera, S., Kohiyama, M., Maki, N. and Fujita, H., 1999. Use of DMSP-OLS images for early identification of impacted areas due to the 1999 Marmara earthquake disaster, *Proceedings of the 20th Asian Conference on Remote Sensing*, Hong Kong, 1291-1296.
- Huyck, C.K. and Adams, B.J., 2002. *Emergency Response in the Wake of World Trade Center Attacks: The Remote Sensing Perspective*, MCEER: Buffalo
- International Charter, 2003. The Charter in Action, http://www.disasterscharter.org/disasters_e.html (accessed 5 Feb. 2004)
- Kohiyama, M., Hayashi, H., Maki, N. and Hashitera, S., 2001. Night Time Damage Estimation, <http://www.gisdevelopment.net/magazine/gisdev/2001/mar/ntde.shtml> (accessed 5 Feb 2004)
- Matsuoka, M. and Yamazaki, F., 1998. Identification of damaged areas due to the 1995 Hyogoken-Nanbu earthquake using satellite optical images, *Proceedings of the 1998 Asian Conference on Remote Sensing*, <http://www.gisdevelopment.net/aars/acrs/1998/ps2/ps2009.shtml> (accessed 5 Feb. 2004)
- Mitomi, H., Matsuoka, M. and Yamazaki, F., 2002. Application of automated damage detection of buildings by panchromatic television images, *Proceedings of the 7th National US Conference on Earthquake Engineering*, Boston.
- NOAA, 2003. National Weather Service Radar Detects Columbia Space Shuttle Disaster, <http://www.crh.noaa.gov/ncrfc/News/news-index.html> (accessed 5 Feb 2004)
- OCHA, 2003. *Algeria – Earthquake OCHA Situation Report No. 9*, <http://www.cidi.org/disaster/03a/ixl143.html> (accessed 5 Feb. 2004)
- Ogawa, N. and Yamazaki, F., 2000. Photo-interpretation of buildings damage due to earthquakes using aerial photographs, *Proceedings of the 12th World Conference on Earthquake Engineering*, Auckland.
- Rathje, E., 2000. Strong ground motions and site effects, In Youd, T.L., Bardet, J.P. and Bray, J.D. (eds.) *Earthquake Spectra Supplement A to Volume 16: Kocaeli, Turkey Earthquake of August 17, 1999 Reconnaissance Report*. MCEER, Buffalo, pp. 65-96.
- Yamazaki, F., Kouchi, K., Kohiyama, M. and Matsuoka, M., 2004. Damage detection for the 2003 Algeria earthquake from Quickbird images, *Proceedings of the 2003 workshop on U.S. Japan Cooperative Research for Urban Earthquake Disaster Mitigation*, Los Angeles.

6. ACKNOWLEDGEMENTS

The author gratefully acknowledges the National Science Foundation and MCEER (NSF Award Number EEC-9701471) for funding this research. Appreciation is extended to: the EERI Learning from Earthquakes Program, for purchasing Quickbird imagery of Boumerdes; the European Space Agency for supplying ERS data, and NIK Insaat Ltd. of Istanbul for providing SPOT coverage of Golcuk; the Architectural Institute of Japan and Professor Fumio Yamazaki of Chiba University, for use of the Golcuk and Boumerdes building damage observations. Sincere thanks are given to Charles K. Huyck and Ronald T. Eguchi of ImageCat, Inc. for their guidance and assistance with damage map and damage profile development. Dr. Babak Mansouri is acknowledged for contributions to the Marmara analysis, together with Dr. Bijan Houshmand from UCLA and Professor Masanobu Shinozuka of UCI.